ARI-RR-1072

LABORATORY STUDIES OF CHEMICAL
AND PHOTOCHEMICAL PROCESSES
RELEVANT TO STRATOSPHERIC OZONE

Second Annual Report
May 1993 - April 1994

Prepared by

Mark S. Zahniser, David D. Nelson, Douglas R. Worsnop and Charles E. Kolb
Center for Chemical and Environmental Physics
Aerodyne Research, Inc.
45 Manning Road
Billerica MA 01821-3976
(508) 663-9500

Prepared for

April 1994

TABLE OF CONTENTS

1. RESEARCH OBJECTIVES

The purpose of this project is to reduce the uncertainty in several key gas-phase kinetic processes which impact our understanding of stratospheric ozone. The main emphasis of this work is on measuring rate coefficients and product channels for reactions of HO_x and NO_x species in the temperature range 200 K to 240 K relevant to the lower stratosphere. Other areas of study have included infrared spectroscopic studies of the HO_2 radical, measurements of OH radical reactions with alternative fluorocarbons, and determination of the vapor pressures of nitric acid hydrates under stratospheric conditions. The results of these studies will improve models of stratospheric ozone chemistry and predictions of perturbations due to human influences.

In this annual report we focus on our recent accomplishments in the quantitative spectroscopy of the HO_2 radical. This work has been accepted for publication and should appear in the literature shortly.

2. SUMMARY OF PROGRESS AND RESULTS

2.1 Spectroscopy of the HO_2 Radical

We have measured the air broadening coefficient for one of the strongest infrared absorption lines of the hydroperoxyl radical - the $9_{19} \leftarrow 8_{18}$ F_1,F_2 doublet of the v_2 band at 1411.18 cm^{-1}. We obtain a value of b = 0.107$\pm$0.009 cm^{-1} atm^{-1} (half-width at half maximum) for the Lorentz broadening caused by air at 296 K. This measurement was made using a high resolution tunable diode laser. The HO_2 was made at atmospheric pressure from the H + O_2 association reaction. The HO_2 was sampled by a fast flow reduced pressure multipass absorption cell using an astigmatic off axis resonator. The optical pathlength was 100 meters with 182 passes. The results of this measurement are essential for the design and implementation of several atmospheric hydroperoxyl monitoring schemes.

2.2 Thermodynamic Studies of Nitric Acid Hydrates at Stratospheric Temperatures

We have continued our studies of nitric acid hydrates relevant to polar stratospheric cloud formation. Formation of crystalline phases of H_2SO_4, HNO_3 and H_2O were studied at stratospheric temperatures and vapor pressures. Freezing of supercooled solutions began at < 200 K by crystallization of $x \cdot H_2SO_4 \cdot HNO_3 \cdot H_2O$, where x is presently undetermined, followed by a progression of metastable phases: [$H_2SO_4 \cdot H_2O$ + $x \cdot H_2SO_4 \cdot HNO_3 \cdot H_2O$ + solution] $\rightarrow$(fast) {$H_2SO_4 \cdot 4H_2O$ + $H_2SO_4 \cdot 6.5H_2O$ + $HNO_3 \cdot 2H_2O$] $\rightarrow$(slow) [$H_2SO_4 \cdot 4H_2O$ + $H_2SO_4 \cdot 6.5H_2O$ + $HNO_3 \cdot 3H_2O$]. Metastable $HNO_3 \cdot 3H_2O$ formed in some experiments. Large particles are readily produced from metastable phases, providing a mechanism for removal of HNO_3. Mixed crystals partially melted at 200 K, forming [$H_2SO_4 \cdot 4H_2O$ + ternary solution], a potentially important process in the arctic polar vortex.

This work is currently being prepared for publication.

2.3 HO_2 Radical Reaction Kinetic Studies

We are continuing our studies of the reactions of HO_2 with NO and O_3. Modifications to the discharge flow system have been implemented to improve temperature control and the detection sensitivity for HO_2 using infrared tunable laser absorption. These studies will be the major emphasis in the coming year of this project.

2.4 Journal Publications

D.D. Nelson and M.S. Zahniser, "A Mechanistic Study of the Reaction of HO_2 Radical with Ozone," J. Phys. Chem. 98, 2101 (1994).

D.D. Nelson and M.S. Zahniser, "Pressure Broadening Measurements of the v_2 Band of the HO_2 Radical," J. Mol. Spec., xx, xxxx (1994).

L.E. Fox, D.R. Worsnop, M.S. Zahniser and S.C. Wofsy, "Non-equilibrium Phases in Polar Stratospheric Aerosols," Science (Manuscript in preparation).

3. HO$_2$ RADICAL SPECTROSCOPY

3.1 Introduction

The hydroperoxyl radical (HO$_2$) participates in the formation and destruction of ozone in both the troposphere and the stratosphere. Together with the hydroxyl radical (OH) it forms catalytic cycles which result in the oxidation of compounds released at the surface of the earth and thus provides the major cleansing mechanism for hydrocarbons and manmade pollutants in the lower atmosphere (1-2). There is, therefore, great interest in direct measurements of the concentration and distribution of HO$_2$ radical throughout the atmosphere.

The various techniques under development for the measurement of HO$_2$ radicals in the troposphere and stratosphere have been reviewed by Cantrell and coworkers (3) and have been the subject of a recent workshop in HO$_x$ measurements. Quantitative spectroscopic approaches, like tunable diode laser absorption (4) and rotational emission spectroscopy (5), have the advantages of species specificity and of an absolute calibration standard. Both of these methods requires accurate line positions, strengths and air broadening factors. The air broadening factors are needed since these are high resolution techniques which resolve individual lines. Line positions (6-11) and strengths (12-15) have been extensively studied for the HO$_2$ radical but its broadening coefficients have not been studied until very recently. In this work we present our measurements of the room temperature air broadening coefficient for the $9_{19} \leftarrow 8_{18}$ F$_1$,F$_2$ doublet of the ν_2 vibrational band at 1411.18 cm^{-1}. This particular line was chosen because it is one of the strongest infrared absorption features available for monitoring the hydroperoxyl radical.

3.2 Experimental

The optical layout and signal processing schematic for our tunable diode laser (TDL) system is shown in Figure 1 and discussed in more detail elsewhere (4). The laser diode is housed in a liquid nitrogen cooled dewar. Laser output is collected with a reflecting microscope objective and focused to a 100 μm pinhole with a 15:1 magnification. The infrared beam is combined with a visible alignment beam from a helium-neon laser using a dichroic mirror which reflects the infrared and transmits the visible light. The pinhole, which is mounted on a removable kinematic base, is used to assure that the two beams are co-aligned at the source. Alignment of the infrared beam through the rest of the optical system is then trivial.
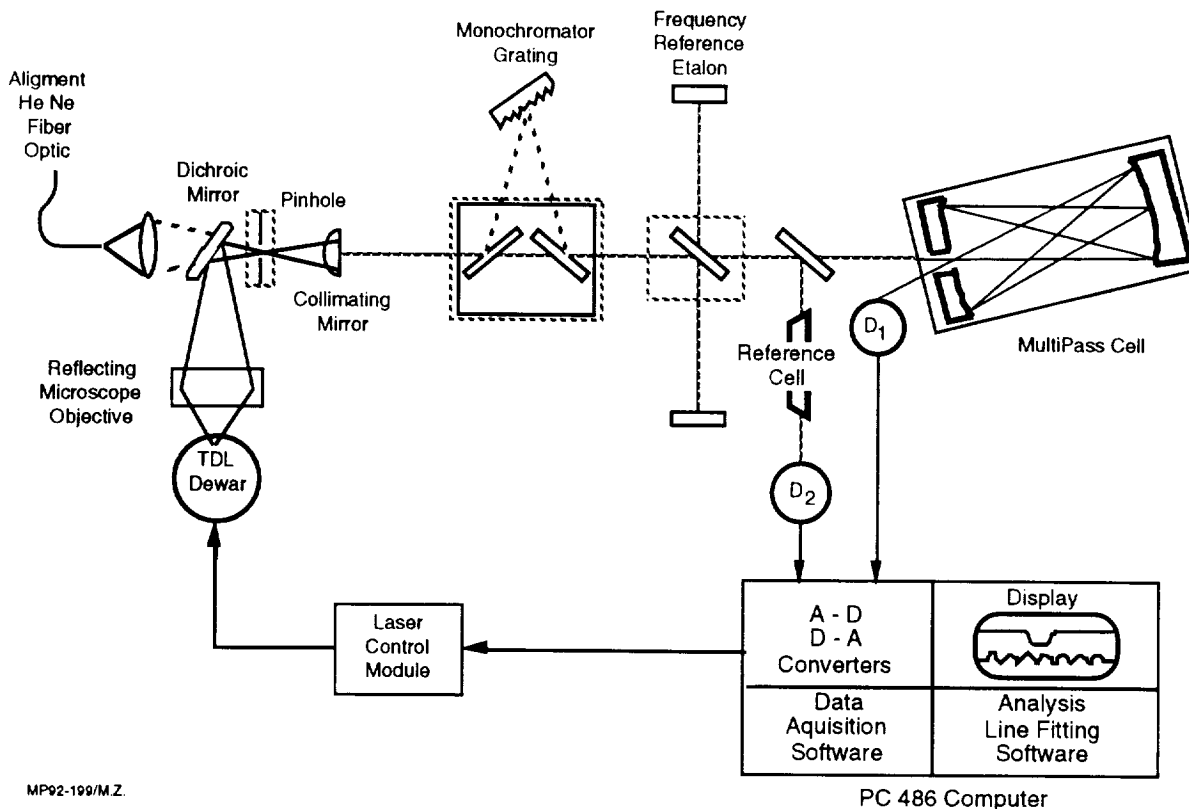
Figure 1. Block Diagram of TDL Absorption System

The beam is collimated with a 2.5 cm diameter spherical mirror. Laser modes are selected, if necessary, with a removable pair of mirrors which deflect the beam to a diffraction grating. A removable beam splitter and two flat mirrors spaced 75 cm apart form a simple yet effective etalon fringe pattern with a free spectral range of 0.0066 cm^{-1} which is used for relative frequency calibration. A second beam splitter and a reference gas cell provide absolute frequencies from known line positions. The beam then enters a multi-pass cell and exits to the main detector.

The multipass cell used is a variation on the design suggested by Herriott and Schulte (16). In this variation astigmatic mirrors are employed to minimize the cell volume for a given pathlength. The two radii of curvature produce beam spots on the mirrors which form a Lissajous pattern, as shown in Figure 2, rather than the elliptical patterns formed by spherical mirrors in the conventional Herriott cell (17). The optical path, therefore, better fills in the optical absorption volume. Thus the astigmatic Herriott cell can have a smaller volume for a given pathlength than spherical mirror cells.
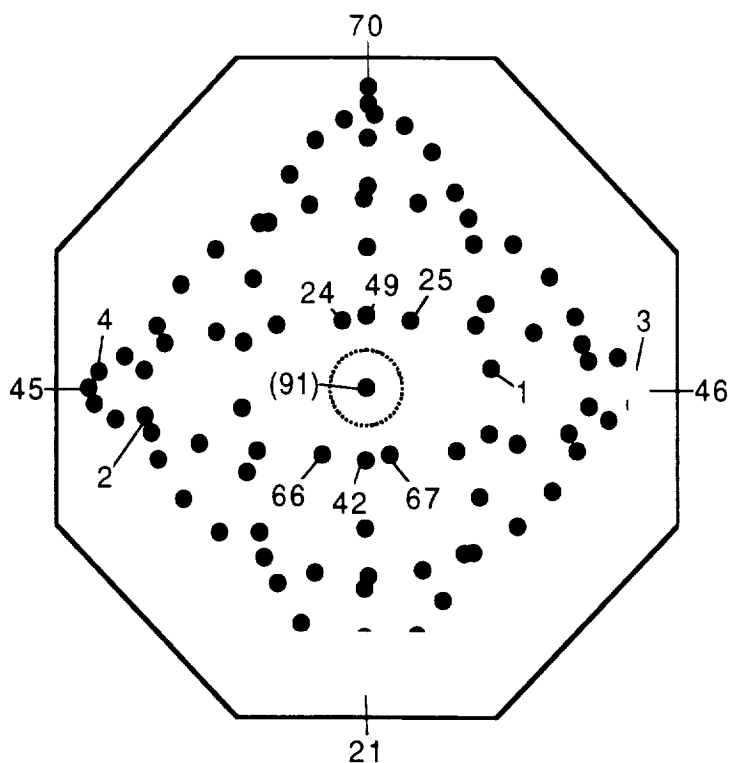
5

Figure 2. Spot Patterns on Astigmatic Mirrors for the 182 Pass, 100 Meter Design

We have designed and constructed such a cell based on a particularly favorable combination of curvatures to produce 182 passes before exiting (18). The cell has a 55 cm base length which gives a path length of 100 meters. With 7.6 cm diameter mirrors, the enclosed volume is 3 liters. The mirrors have a reflectivity of 99.1% from 3 to 10 μm resulting in a 20% transmission of light through the cell.

A set of mirrors based on this design was installed in a cell designed for rapid throughput and fast response that makes it ideal for spectroscopic studies of transient species like HO_2. The radical sampling cell and HO_2 source are shown in Figure 3. A 100 m astigmatic Herriott cell is contained within a low volume (3 liter) fast response (τ ~300 ms) flow cell. At the inlet to the cell there is a simple atmospheric pressure HO_2 source, consisting of a small gas flow of ~5% H_2 in He which passes through a high pressure microwave discharge cavity (producing H atoms) and then mixes with a large gas flow of either ambient room air or dry bottled air. The association reaction of hydrogen atoms with oxygen molecules to form HO_2 is very fast at atmospheric pressure, and large concentrations of HO_2 (10^{13} - 10^{14} cm^{-3}) are formed just before the cell's inlet

Window

IR Beams In/Out

Filler Block

Pressure Vessel Wall

Glass Liner

Filler Block with Flow Channel

HO_2 Source
$H+O_2 + M$
N_2, O_2

Inlet Nozzle

μ Wave Cavity

He, H_2

Exhaust Pipe

Exhaust Plenum

Input Mirror

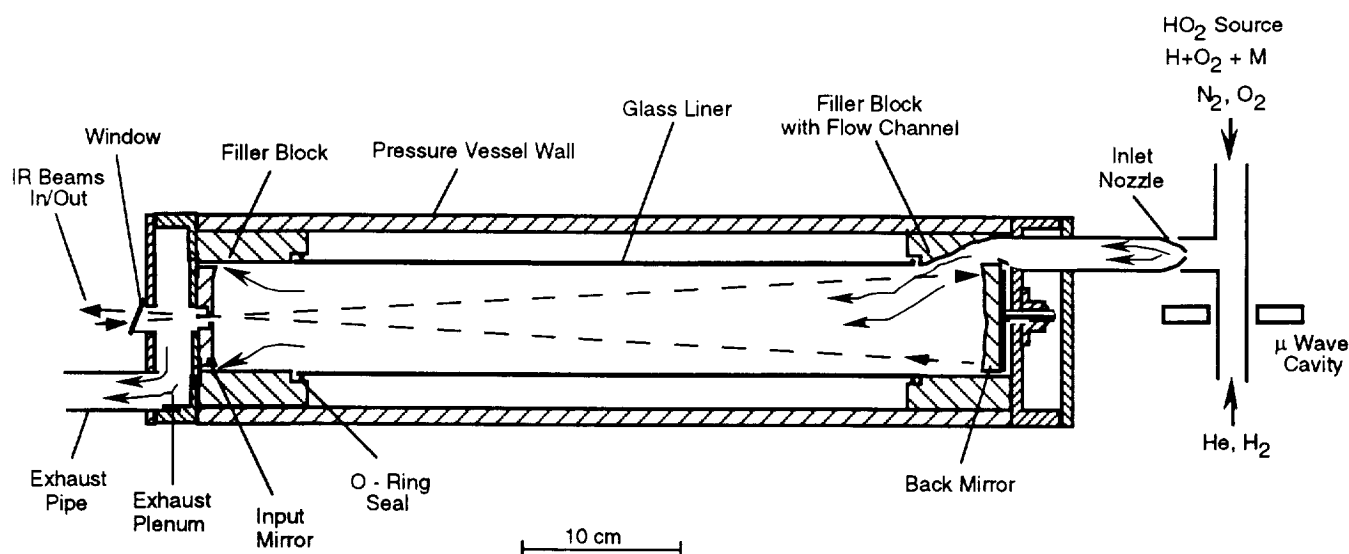O - Ring Seal

Back Mirror

10 cm

MP92-031b/M.Z.

Figure 3. Atmospheric Pressure HO_2 Source Coupled to Fast Response Flow Cell with Astigmatic Herriott Multipass Optics. Optical pathlength = 100 m

nozzle. The radicals then enter the cell through a supersonic orifice with a large pressure drop. For a 20 Torr cell pressure we have measured column densities equivalent to an average $[HO_2]$ of 1×10^{12} cm^{-3}.

The data acquisition method employed in this work is based on rapid sweep integration over the full infrared transition line shape. This is accomplished by scanning the laser frequency under computer control and synchronously measuring the transmitted infrared light intensity. The laser current is dropped below threshold at the end of each scan to obtain the unabsorbed intensity level. This spectral information can be analyzed in real time with a nonlinear least squares fitting routine which returns both the spectral line profile and laser intensity spectrum. The area under the absorption line together with the absorption coefficient for the line is used to calculate the column density of the species being observed.

The nonlinear least squares fitting routine is crucial for absolute absorption measurements and for lineshape studies. The fitting routine uses the Levenberg-Marquardt approach (19). The diode laser intensity spectrum is represented as a slowly varying polynomial of adjustable order; typically a quadratic or cubic polynomial is used. The absorption lineshape may be fit to either a Gaussian, pressure broadened Lorentzian or Voigt profile. The position, width and height of the line are simultaneously fit together with the diode laser polynomial baseline. The absolute accuracy of the area under the peak returned by the fit is a few per cent.

7

3.3 Results

A survey spectrum of HO_2 spanning 1410.9 to 1411.4 cm^{-1} is shown in the upper panel of Figure 4. An HO_2 resolved doublet, coincident doublet, and resolved quartet are seen with peak absorptions of ~2-5%. Also shown is the etalon trace used to calibrate the frequency scale for the pressure broadening measurements. The bottom panel of Figure 4 shows the result of a fit carried out on the spectrum of the coincident doublet ($9_{19} \leftarrow 8_{18}$ F_1,F_2) obtained at 16 Torr. Approximately 1/2 of the linewidth is Gaussian (due to Doppler and instrumental broadening) and ~1/2 is Lorentzian (due to pressure broadening). All of the broadening measurements reported in this work are based on this coincident doublet at 1411.18 cm^{-1}. The pressure was varied by throttling the pump. Spectra were taken at pressures from 5-80 Torr and fit to a Voigt profile using a nonlinear least squares fit as described above. In these fits the doublet was treated as a singlet
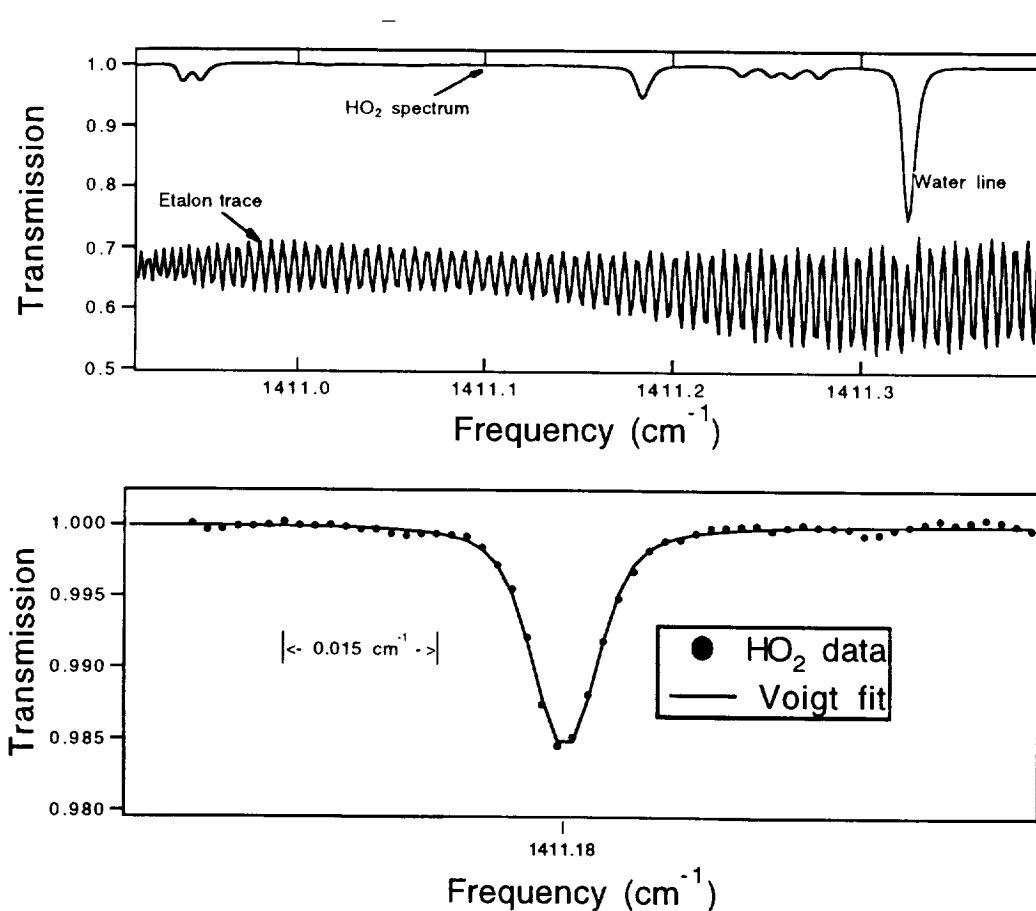

Figure 4. HO_2 Absorption Spectra Obtained in 100 Meter Pathlength Fast Response Flow Cell

since the two components of the doublet differ in frequency by only 0.0004 cm^{-1}. This splitting was completely unobservable even at low pressure, being dominated by the combined effects of Doppler broadening (Γ_{HWHM} = 0.0015 cm^{-1}) and the finite laser linewidth (Γ_{HWHM} ~ 0.0019 cm^{-1}). The laser linewidth appears to be largely Gaussian in nature and is deduced from the observed spectral linewidth (Γ_{HWHM} =0.0024 cm^{-1}) at low pressure. This excess Gaussian broadening is attributed to the laser linewidth. The pressure dependent Voigt profiles were fit with the peak position, peak height and Lorentzian halfwidth floated and the Gaussian halfwidth fixed at 0.0024 cm^{-1}. The reported pressure broadening coefficient is relatively insensitive to the value chosen for the Gaussian halfwidth.

Our results are summarized in Figure 5 where we plot the Lorentzian component of the observed linewidth versus the cell pressure both for room air and dry air. The error bars in Figure 5 are the 95% confidence limits derived from the random errors in the nonlinear least
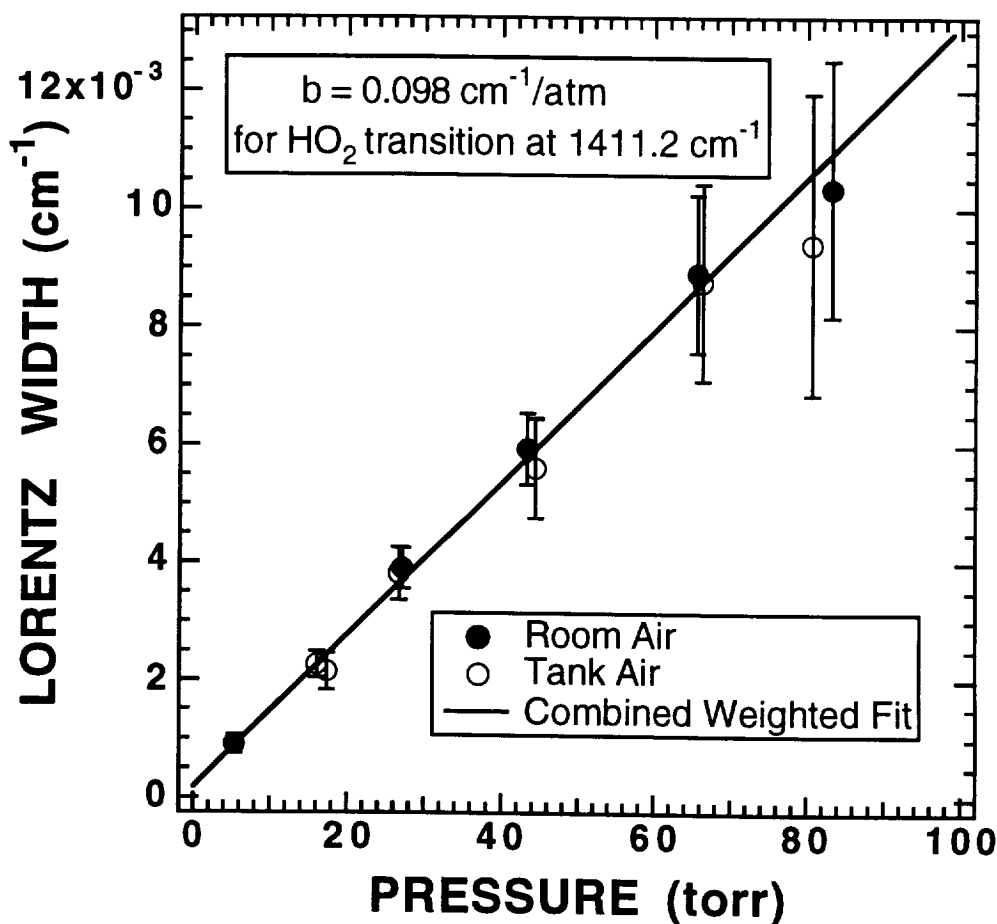

Figure 5. HO$_2$ Air Broadened Linewidth Measurements in a Mixture of 86.5% air, 13.5% Helium and 0.5% Hydrogen

squares fits. Since there is no significant difference between the two data sets, they were fit together. This is not surprising since the water vapor mixing ratio in the cell was only 2.7 parts per thousand. The eleven observed halfwidths were fit to a straight line using a least squares fit weighted by the inverse of the plotted uncertainties. The slope of the fit line implies a broadening coefficient of 0.098 ± 0.007 cm^{-1} atm^{-1} (HWHM) for the gas mixture. The Lorentz halfwidth at zero pressure is determined as 0.0002 ± 0.0002 cm^{-1}. The reported uncertainties represent 95% confidence limits with respect to random errors. The mixture employed was 86.5% air, 13% He and 0.5% H_2. It was difficult to vary this mixture substantially while maintaining sufficient HO_2 signal for pressure broadening studies. However, the He and H_2 concentrations were small enough that we can still report a fairly precise air broadening coefficient. We ignore the H_2 pressure broadening since H_2 is only present in trace quantities. To correct for the presence of He we note that the weakly interacting He atom is likely to be a much less efficient line broadener than either N_2 or O_2. In fact, the air broadening coefficients of OH rotational transitions are ~5x larger than the He broadening coefficients (20). We therefore assume that the He broadening coefficient with HO_2 is one third of the air broadening coefficient and we increase our reported uncertainties in the air broadening coefficients to allow for He broadening coefficients between 0 and 2/3 of the air broadening values. This implies an air broadening coefficient of 0.107 ± 0.009 cm^{-1} atm^{-1} for the $9_{19} \leftarrow 8_{18}$ F_1,F_2 doublet (1411.180 cm^{-1}) in the v_2 band.

3.4 Discussion

The line broadening coefficient reported in this work has direct implications for the design and interpretation of atmospheric monitoring experiments for the hydroperoxyl radical. The two obvious implications are: 1) the broadening coefficient determines the maximum line center absorption for a given linestrength, and 2) it determines the optimal pressure for reduced pressure sampling in the infrared absorption approach.

We are aware of three previous HO_2 pressure broadening measurements. Unfortunately, none of these studies can be directly compared as they each monitored different transitions. The earliest measurement is that of Hayman and Jenkin (21) who obtained 0.106 ± 0.008 cm^{-1} atm^{-1} with N_2 and 0.071 ± 0.01 cm^{-1} atm^{-1} with O_2 broadening of the $6_{15} \leftarrow 5_{14}$ F_1 (1110.287 cm-1) line in the v_3 band of HO_2. These numbers would correspond to a broadening coefficient for air of 0.099 ± 0.01 cm^{-1} atm^{-1}. Their result is similar to ours, but applies to a somewhat lower rotational transition in the v_3 band.

Johnson et al. (22) measured an air broadening coefficient for an unidentified HO_2 line in the $2v_1$ overtone band at 1.5 μm wavelength. Their value is only approximate due to the difficulty

of deconvolving the Voigt profile from the second harmonic signal obtained using their two tone frequency modulation signal processing method. Their result appears to be consistent with ours but is not well enough defined to provide a strong check.

Recently, Chance and coworkers ([23]) have measured the room temperature oxygen and nitrogen pressure broadening coefficients for the $13_{2,12} \leftarrow 12_{1,11}$ F_1 pure rotational transition of HO_2. Their results imply an air broadening coefficient for this transition of 0.141 ± 0.012 cm^{-1} atm^{-1}. This value is approximately 30% larger than that which we obtain for the $9_{19} \leftarrow 8_{18}$ F_1, F_2 doublet in the v_2 infrared band. We find the difference between these two measurements to be surprising. In general, the vibrational dependence of pressure broadening coefficients is found to be small. In addition, these coefficients often decrease slightly with increasing J and K for moderate values of J. Hence, we might expect the broadening coefficient for the pure rotational transition to be slightly smaller than that of the infrared transition studied in this work - not significantly larger as observed. It is not clear whether this implies an error in one of the measurements. Exceptions to the usual trends for pressure broadening coefficients have been noted in other systems ([24]). In addition, it is conceivable that line mixing effects may play a role in the relative narrowness of the infrared transition since it does consist of two components which are unresolved even at zero pressure. However, we consider this possibility to be unlikely since the two lines belong to separate spin rotation manifolds which are only weakly connected by electric dipole transitions. It therefore seems unlikely that collisional transfer could be effective enough to cause significant coherence transfer.

Further work on the HO_2 radical should certainly explore the rotational and vibrational dependence of the broadening coefficients. In addition, measurement of the temperature dependence of theses coefficients will be very important since lower stratospheric and upper tropospheric temperatures are often 200 K or lower. Direct monitoring of the HO_2 radical in these environments will potentially require a large temperature correction to the room temperature broadening coefficients.

3.5 References

1. P.J. Crutzen, The Major Biogeochemical Cycles and Their Interactions; B. Bolin and R.B. Cook, eds., 68-114, John Wiley and Sons, Chichester UK (1983).

2. J.A. Logan, *J. Geophys. Res.* **90**, 10463-10482 (1985).

3. C.A. Cantrell, R.E. Shetter, A.H. McDaniel and J.G. Calvert, ACS Advances in Chemistry Series, American Chemical Society (1991).

4. D.R. Worsnop, D.D. Nelson and M.S. Zahniser, SPIE, **1715**, 18-33 (1992).

5.   W.A. Traub, D.G. Johnson, and K.V. Chance, *Science*, **247**, 446-449 (1990).

6.   J.W.C. Johns, A.R.W. McKellar, and M. Riggin, *J. Chem. Phys.* **68**, 3957-3966 (1978).

7.   K. Nagai, Y. Endo and E. Hirota, *J. Mol. Spectrosc.* **89**, 520-527 (1981).

8.   A. Charo, and F.C. DeLucia, *J. Mol. Spectrosc.* **94**, 426-436 (1982).

9.   C. Yamada, Y. Endo and E. Hirota, *J. Chem. Phys.* **78**, 4379-4384 (1983).

10. D.D. Nelson, Jr. and M.S. Zahniser, *J. Mol. Spectrosc.* **150**, 527-534 (1991).

11. J.B. Burkholder, P.D. Hammer and C.J. Howard, *J. Mol. Spectrosc.* **151**, 493-512 (1992).

12. S. Saito, and C. Matsumura, *J. Mol. Spectrosc.* **80**, 34-40 (1980).

13. T.T. Paukert and H.S. Johnson, *J. Chem. Phys.* **56**, 2824-2838 (1972).

14. J.W. Buchanan, B.A. Thrush and G.S. Tyndall, *Chem. Phys. Lett.* **103**, 167-168 (1983).

15. M.S. Zahniser, K.E. McCurdy and A.C. Stanton, *J. Phys. Chem.* **93**, 1065-1070 (1989).

16. D.R. Herriott, and H.J. Schulte, Jr., *Appl. Optics* **4**, 883-889 (1965).

17. D.R. Herriott, H. Kogelnik and R. Kompfer, *Appl. Optics* **3**, 523-526 (1964).

18. J.B. McManus, P.L. Kebabian and M.S. Zahniser, to be submitted to *Appl. Optics* (1994).

19. W.H. Press, B.P. Flannery, S.A. Teukolsky and W.T. Vetterling, Numerical Recipes; 521-538, Cambridge University Press, Cambridge UK, (1986).

20. K.V. Chance, D.A. Jennings, K.M. Evenson, M.D. Vanek, I.G. Nolt and J.V. Radostitz, *J. Mol. Spectrosc.* **146**, 375-380 (1991).

21. G.D. Hayman and M.E. Jenkin, Abstract. Personal communication (1992).

22. T.J. Johnson, F.G. Wienhold, J.P. Burrows, G.W. Harris and H. Bughhand, *J. Phys. Chem.* **95**, 6499-6502 (1991).

23. K. Chance, P. De Natale, M. Bellini, M. Inguscio, G. Di Lonardo and L. Fusina, *J. Mol. Spectrosc.* **163**, 67-70 (1994).

24. R.R. Gamache and L.S. Rothman, *Appl. Optics* **24**, 1651-1656 (1985).

Report Documentation Page

1. Report No.	2. Government Accession No.	3. Recipient's Catalog No.

4. Title and Subtitle	5. Report Date
Laboratory Studies of Chemical and Photochemical Processes Relevant to Stratospheric Ozone	April 1994
	6. Performing Organization Code

7. Author(s)	8. Performing Organization Report No.
M.S. Zahniser, D.D. Nelson, D.R. Worsnop and C.E. Kolb	ARI-RR-1072
	10. Work Unit No.

9. Performing Organization Name and Address	11. Contract or Grant No.
Aerodyne Research, Inc. 45 Manning Road Billerica, MA 01821-3976	NAS5-31847
	13. Type of Report and Period Covered
12. Sponsoring Agency Name and Address	Annual May 1993 – April 1994
National Aeronautics and Space Administration Washington, DC 20546-0001	14. Sponsoring Agency Code

15. Supplementary Notes

Louis Stief, Contract Monitor

16. Abstract The purpose of this project is to reduce the uncertainty in several key gas-phase kinetic processes which impact our understanding of stratospheric ozone. The main emphasis of this work is on measuring rate coefficients and product channels for reactions of HO_x and NO_x species in the temperature range 200 K to 240 K relevant to the lower stratosphere. Other areas of study have included infrared spectroscopic studies of the HO_2 radical, measurements of OH radical reactions with alternative fluorocarbons, and determination of the vapor pressures of nitric acid hydrates under stratospheric conditions. The results of these studies will improve models of stratospheric ozone chemistry and predictions of perturbations due to human influences.

In this annual report we focus on our recent accomplishments in the quantitative spectroscopy of the HO_2 radical. This report details the measurements of the broadening coefficients for the ν_2 vibrational band.

Further measurements of the vapor pressures of nitric acid hydrates relevant to the polar stratospheric cloud formation indicate the importance of metastable crystalline phases of H_2SO_4, HNO_3 and H_2O. Large particles produced from these metastable phases may provide a removal mechanism for HNO_3 in the polar stratosphere.

17. Key Words (Suggested by Author(s))	18. Distribution Statement
hydroperoxyl radical, ozone, stratosphere, kinetics, nitric acid hydrates	UNCLASSIFIED UNLIMITED

19. Security Classif. (of this report)	20. Security Classif. (of this page)	21. No. of pages	22. Price
UNCLASSIFIED	UNCLASSIFIED	12	